Anisotropy of the Seebeck Coefficient in the Cuprate Superconductor $YBa_2Cu_3O_y$: Fermi-Surface Reconstruction by Bidirectional Charge Order

O. Cyr-Choinière,[1,†] S. Badoux,[1] G. Grissonnanche,[1] B. Michon,[1] S. A. A. Afshar,[1] S. Fortier,[1] D. LeBoeuf,[2] D. Graf,[3] J. Day,[4] D. A. Bonn,[4,5] W. N. Hardy,[4,5] R. Liang,[4,5] N. Doiron-Leyraud,[1] and Louis Taillefer[1,5,*]

[1]*Institut quantique, Département de physique and RQMP, Université de Sherbrooke, Sherbrooke, Québec J1K 2R1, Canada*

[2]*Laboratoire National des Champs Magnétiques Intenses, UPR 3228, (CNRS-INSA-UJF-UPS), Grenoble 38042, France*

[3]*National High Magnetic Field Laboratory, Tallahassee, Florida 32310, USA*

[4]*Department of Physics and Astronomy, University of British Columbia, Vancouver, British Columbia V6T 1Z4, Canada*

[5]*Canadian Institute for Advanced Research, Toronto, Ontario M5G 1Z8, Canada*

(Received 17 April 2017; revised manuscript received 30 June 2017; published 12 September 2017)

The Seebeck coefficient S of the cuprate $YBa_2Cu_3O_y$ is measured in magnetic fields large enough to suppress superconductivity, at hole dopings $p = 0.11$ and $p = 0.12$, for heat currents along the a and b directions of the orthorhombic crystal structure. For both directions, S/T decreases and becomes negative at low temperature, a signature that the Fermi surface undergoes a reconstruction due to broken translational symmetry. Above a clear threshold field, a strong new feature appears in S_b, for conduction along the b axis only. We attribute this feature to the onset of 3D-coherent unidirectional charge-density-wave modulations seen by x-ray diffraction, also along the b axis only. Because these modulations have a sharp onset temperature well below the temperature where S/T starts to drop towards negative values, we infer that they are not the cause of Fermi-surface reconstruction. Instead, the reconstruction must be caused by the quasi-2D bidirectional modulations that develop at significantly higher temperature. The unidirectional order only confers an additional anisotropy to the already reconstructed Fermi surface, also manifest as an in-plane anisotropy of the resistivity.

DOI: 10.1103/PhysRevX.7.031042

Subject Areas: Condensed Matter Physics, Strongly Correlated Materials, Superconductivity

I. INTRODUCTION

In the past decade, various transport measurements in high magnetic fields have revealed that the Fermi surface of hole-doped cuprate superconductors undergoes a reconstruction at low temperature in a doping interval centered at $p \simeq 0.12$ [1]. The key feature of this Fermi-surface reconstruction (FSR) is the presence of a small electronlike pocket, detected by quantum oscillations [2–5], combined with sign changes in the temperature dependence of the Hall (R_H) and Seebeck (S) coefficients, from positive at high temperature to negative at low temperature. A negative R_H or S has now been observed in seven hole-doped cuprates: $YBa_2Cu_3O_y$ (YBCO) [6–9], $YBa_2Cu_4O_8$ (Y124) [6], $HgBa_2CuO_{4+\delta}$ (Hg1201) [10], $La_{2-x}Sr_xCuO_4$ (LSCO) [11,12], $La_{1.8-x}Eu_{0.2}Sr_xCuO_4$ (Eu-LSCO) [9], $La_{1.6-x}Nd_{0.4}Sr_xCuO_4$ (Nd-LSCO) [13,14], and $La_{2-x}Ba_xCuO_4$ (LBCO) [15].

There is compelling evidence that this FSR is caused by charge-density-wave (CDW) order. Indeed, in all materials and at every doping where FSR has been detected, CDW modulations have also been observed by x-ray diffraction (XRD) [16–21] (except in Y124, where no XRD search has been reported). Having said this, the mechanism by which CDW order produces a small electron pocket in the Fermi surface of hole-doped cuprates remains a puzzle. This is because CDW order is thought to be unidirectional (or "stripelike") in at least some cuprates, and a unidirectional CDW modulation does not, in general, produce a closed electron pocket [22], at least not at "nodal" locations in the Brillouin zone, away from the antinodal pseudogap [23]. By contrast, bidirectional CDW order (with in-plane modulations along both high-symmetry directions of the tetragonal or orthorhombic lattice) readily produces a closed electron pocket at nodal locations [24,25].

This paradox has recently become vivid in the orthorhombic cuprate YBCO at $p = 0.12$, where XRD studies in

*louis.taillefer@usherbrooke.ca

†Present address: Department of Physics, McGill University, Montreal, Québec H3A 2T8, Canada.

high magnetic fields detect long-range three-dimensional CDW order [26], with modulations that run only along the b axis [27,28], above a sharply defined threshold field that coincides with an anomaly in the sound velocity considered to be the thermodynamic signature of CDW order in YBCO [29]. Is this field-induced unidirectional CDW order causing the FSR in YBCO?

Here, we report measurements of the Seebeck coefficient S of YBCO along the a and b axes at $p = 0.11$ and $p = 0.12$, in magnetic fields high enough to reach the normal state. For both directions, we observe a negative S at low temperature, the signature of a FSR that produces an electron pocket. In addition, we detect a pronounced minimum in $S_b(H)$, not present in $S_a(H)$, whose onset field and temperature match the onset of the 3D unidirectional CDW order seen by XRD. However, since this onset temperature is well below the temperature where S/T starts to drop towards negative values, we infer that the primary cause of the FSR is the 2D bidirectional CDW modulations that develop in tandem with the gradual drop in S/T. It appears that the 3D unidirectional order only confers an additional anisotropy to the already reconstructed Fermi surface.

II. METHODS

Single crystals of $YBa_2Cu_3O_y$ are prepared by flux growth [30]. Their hole concentration (doping) p is determined from the superconducting transition temperature T_c [31], defined as the temperature below which the zero-field resistance is zero. A high degree of oxygen order is achieved for samples with $p = 0.11$ ($y = 6.54$, ortho-II order, $T_c = 61.5$ K) and $p = 0.12$ ($y = 6.67$, ortho-VIII order, $T_c = 65.4$ K). The Seebeck coefficient S—the longitudinal voltage generated by a longitudinal thermal gradient—is measured, as described elsewhere [9], on two pairs of a-axis and b-axis YBCO samples, with dopings $p = 0.11$ and $p = 0.12$. $S(H)$ is measured as a function of magnetic field up to $H = 34$ T, applied along the c axis, in YBCO samples with $p = 0.11$ at the Laboratoire National des Champs Magnétiques Intenses (LNCMI) in Grenoble and in samples with $p = 0.12$ at the National High Magnetic Field Laboratory (NHMFL) in Tallahassee. Our b-axis sample with $p = 0.11$ is also measured up to $H = 45$ T, at the NHMFL.

The resistivity ρ is also measured at $p = 0.12$ for both in-plane directions, up to 45 T at the NHMFL. At $p = 0.11$ and 0.12, the critical field for suppressing superconductivity in YBCO is $H_{c2} \simeq 25$ T [32]. Superconducting fluctuations persist up to roughly 30 T, as detected by the nonlinear field dependence of the Nernst [8] and magnetization [33] signals.

III. RESULTS

In Fig. 1, the Seebeck coefficient of YBCO at $p = 0.11$ is plotted as S/T versus H, for several temperatures. Our data on S_a agree well with previous measurements of the Seebeck coefficient in YBCO [8,9]. To our knowledge, there are no prior high-field measurements of S_b in YBCO. We see that for both directions, S/T at high field goes from positive at high temperature to negative at low temperature, the signature that FSR is occurring upon cooling, resulting in a Fermi surface at low temperature that contains a small electron pocket [1]. Note that the magnitude of S/T at $T \to 0$ ($\simeq -0.8$ $\mu V/K^2$) is consistent with theoretical expectation [34] in the sense that $S/T = -(\pi^2/2)(k_B/e)(1/T_F) = -1.0$ $\mu V/K^2$ [9], if we use the Fermi temperature $T_F = 410$ K measured by quantum oscillations in YBCO at $p = 0.11$ [2,35].

The isotherms of S_b in Fig. 1(b) reveal a new and pronounced feature, essentially absent in S_a. Indeed, on top of the same overall field and temperature dependence as

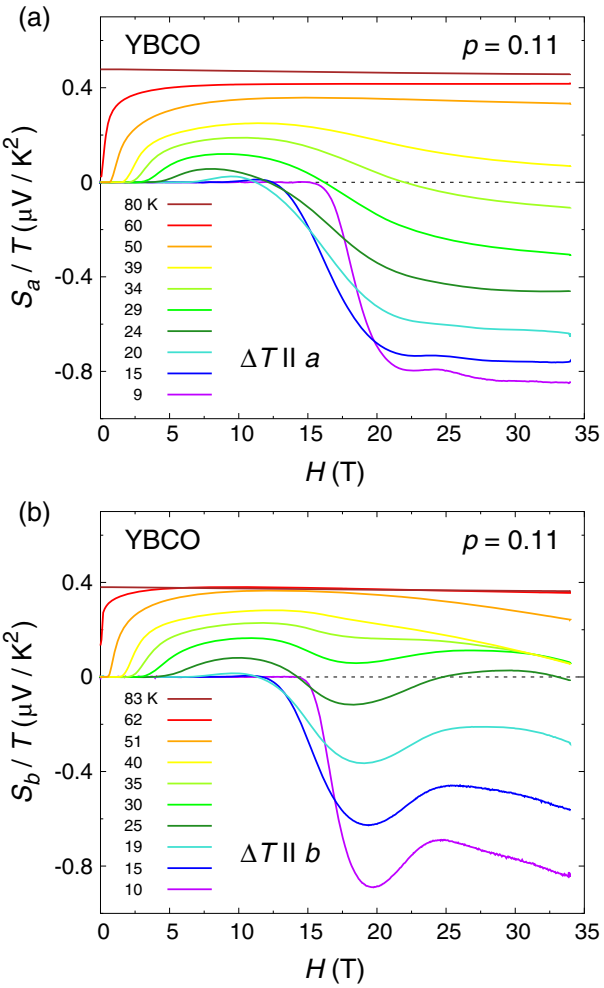

FIG. 1. Seebeck coefficient of YBCO at $p = 0.11$, for a heat current along the a axis (a) and b axis (b) of the orthorhombic crystal structure, plotted as S/T versus magnetic field H, at various temperatures, as indicated. The negative value of S/T at low temperature and high field is the signature of Fermi-surface reconstruction. In the isotherms of S_b/T versus H (b), a clear dip develops below $T \simeq 40$ K, at $H \simeq 18$ T.

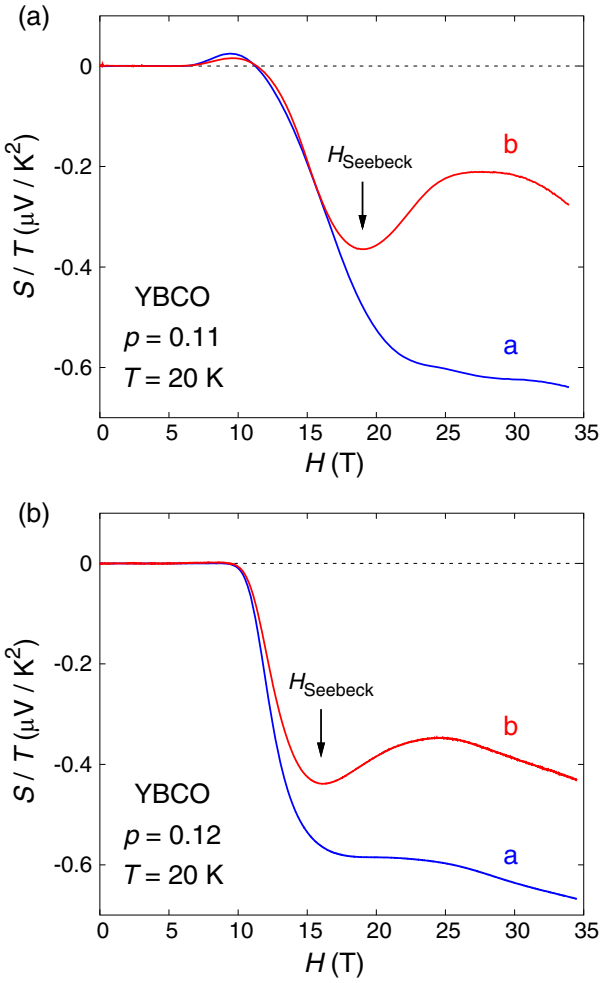

FIG. 2. Seebeck coefficient of YBCO along the a axis (blue line) and b axis (red line) at $T = 20$ K, for $p = 0.11$ (a) and $p = 0.12$ (b), plotted as S/T versus magnetic field H. At both dopings, the Seebeck coefficient exhibits a strong anisotropy, manifest as an upturn in S_b above H_{Seebeck} (arrow).

observed in S_a/T, S_b/T exhibits an upturn at high field, producing a dip at $H \simeq 18$ T that deepens as temperature is reduced. In Fig. 2(a), we focus on this feature by comparing S_a/T (blue line) and S_b/T (red line) versus H at $T = 20$ K. At low field (up to about 16 T), both curves are identical: zero in the vortex-solid state, then slightly positive, followed by a dramatic drop to large negative values. At fields above 16 T, a striking anisotropy between the two directions appears, as a pronounced upturn develops in S_b, but not in S_a. We identify the field at which S_b reaches a minimum as H_{Seebeck}, equal to 19 ± 1 T at $T = 20$ K. Figure 2(b) presents the same comparison at $p = 0.12$, in crystals with a different oxygen order (ortho-VIII instead of ortho-II). We observe a very similar Seebeck anisotropy, again characterized by an upturn in S_b, appearing above $H_{\mathrm{Seebeck}} = 16 \pm 1$ T.

To study the temperature dependence of H_{Seebeck} in detail, we measure closely spaced isotherms of S_b up to

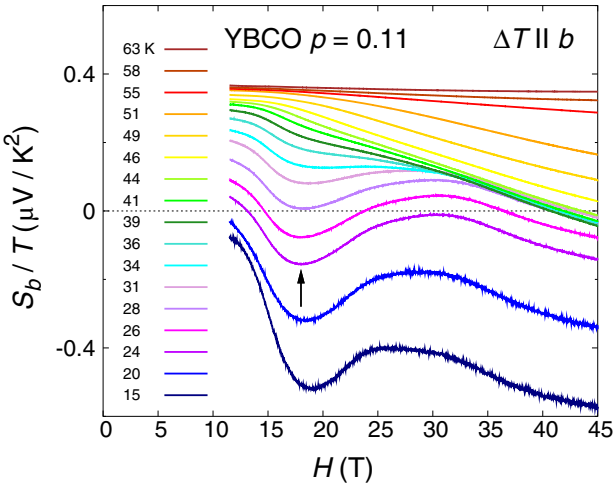

FIG. 3. Seebeck coefficient of YBCO at $p = 0.11$ for a heat current along the b axis, plotted as S/T versus magnetic field H, at various temperatures, as indicated. This more complete data set complements that of Fig. 1(b), showing closely spaced isotherms up to higher field. The arrow marks H_{Seebeck}, whose value is plotted in the H-T phase diagram of Fig. 4. A cut at $H = 34$ T yields the values of S_b/T plotted in Fig. 5(a) (as red dots).

45 T, plotted in Fig. 3. We see that the minimum in S_b/T versus H is present at temperatures up to at least 30 K, remaining in roughly the same position. In Fig. 4, we plot H_{Seebeck} on the H-T phase diagram of YBCO at $p = 0.11$ (yellow squares). It is essentially constant in temperature up to 30 K.

In Fig. 5(a), $S_a(T)$ and $S_b(T)$ measured at $H = 34$ T are compared directly, plotted as S/T versus T. We see that down to 45 K the two curves are approximately parallel, with a roughly constant difference between them. Indeed, a smooth fit through the a-axis data (blue line) makes a good fit through the b-axis data if the line is simply shifted down rigidly (red line). Below 45 K, S_a/T continues its monotonic decrease, but the anomalous feature in S_b produces a striking departure of S_b/T from its fit line (red), initially as a plateau which persists down to $\simeq 30$ K. To capture this extra anisotropy, we plot the difference between b-axis data and red fit line in the inset of Fig. 5(a). We see that it appears below $T_{\mathrm{Seebeck}} = 47 \pm 5$ K. T_{Seebeck} is plotted on the H-T phase diagram of Fig. 4, for three different fields.

IV. DISCUSSION

The anomaly in S_b we observe in YBCO at $p = 0.11$ is confined to a region of the H-T diagram (Fig. 4) that is essentially the same region where 3D unidirectional CDW order has been observed by XRD [26–28]. This order was detected in YBCO above an onset field $H = 18$ T at $p = 0.11$ [28] and above $H = 15$ T at $p = 0.12$ [26,27], in good agreement with $H_{\mathrm{Seebeck}} = 19 \pm 1$ T and 16 ± 1 T at $p = 0.11$ and 0.12, respectively (Fig. 2). This value of H_{Seebeck} at $p = 0.11$ is in agreement with the anomaly in

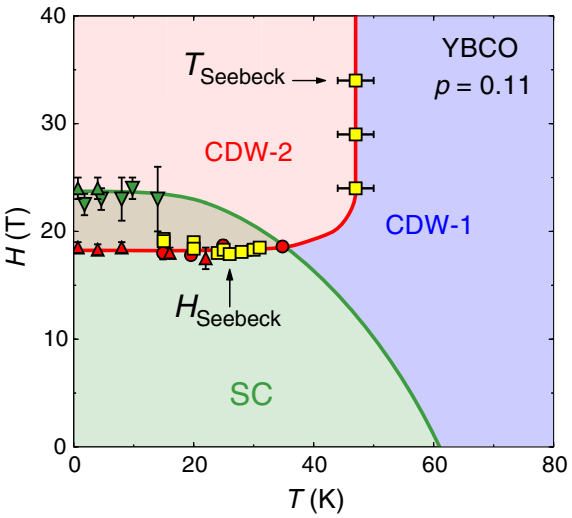

FIG. 4. Magnetic field-temperature phase diagram of YBCO at $p = 0.11$, showing the field H_{Seebeck} (Fig. 3) above which, and the temperature T_{Seebeck} (Fig. 5) below which, the strong anomalous anisotropy in the Seebeck coefficient appears (yellow squares). H_{Seebeck} is seen to coincide with the threshold field detected in the sound velocity (red circles; Ref. [29]) and in the thermal Hall conductivity κ_{xy} (red triangles; Ref. [36]) of YBCO at $p = 0.11$. The upper critical field H_{c2} (green down triangles from Ref. [32], green up triangles from Ref. [36]) is also shown, delineating the superconducting (SC) phase. The green line is a guide to the eye ending at the zero-field T_c. Short-range 2D bidirectional CDW modulations (CDW-1) are detected by XRD throughout this phase diagram, both in the blue region above the red and green lines, as well as below (to the left of) those lines. In addition, long-range 3D unidirectional modulations (CDW-2) are detected in YBCO in a region very similar to the red region defined here, namely, with an onset temperature $T \simeq 47$ K and field $H \simeq 18$ T at $p = 0.11$ [28], and $T \simeq 47$ K and $H \simeq 15$ T at $p = 0.12$ [27]. The red line is a guide to the eye.

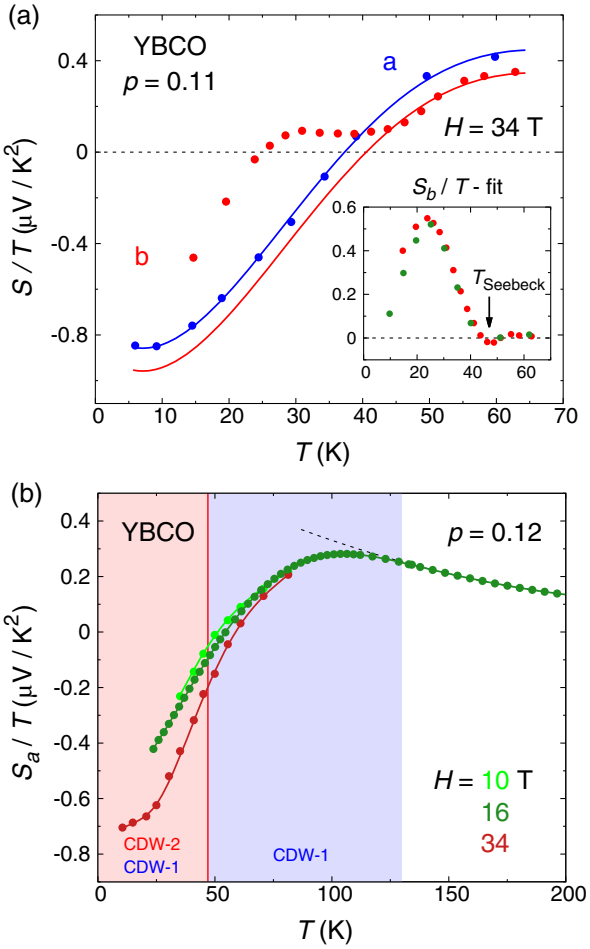

FIG. 5. (a) Seebeck coefficient of YBCO at $p = 0.11$ along the a axis (blue points) and b axis (red points), at $H = 34$ T, plotted as S/T versus T. The blue line is a smooth fit to the S_a data; the red line is the same line shifted down by 0.1 μV/K^2. The anomalous feature seen in the field dependence of S_b (Fig. 2) shows up in the temperature dependence of S_b/T initially as a plateau. Inset: Difference between the b-axis data points and the red line (fit) in the top panel (red dots). The green dots are obtained using the S_b data of Fig. 1(b). The onset temperature for the extra anisotropy is $T_{\text{Seebeck}} = 47 \pm 5$ K (arrow). (b) S_a/T versus T, in YBCO at $p = 0.12$, for three field values as indicated. At all fields, 2D bidirectional CDW modulations (CDW-1) are observed in the blue and red regions [37], while 3D unidirectional CDW order (CDW-2) is observed only in the red region and only when $H > 15$ T [27,28]. The dashed line is a smooth extension of the high-T data below its inflection point at $T = 130$ K. The red line is a smooth guide through the red data points.

the sound velocity [29] that marks the phase transition to CDW order (Fig. 4). Those field values are also in agreement with the threshold field detected in the thermal Hall conductivity κ_{xy} [36], for both $p = 0.11$ (Fig. 4) and $p = 0.12$. Therefore, it is clear that H_{Seebeck} coincides with the onset of 3D unidirectional CDW order.

The onset temperature for that order ($T \simeq 47$ K) [27,28] is not far below the onset of the NMR splitting associated with CDW order [38]. There is little doubt that $T \simeq 47 \pm 5$ K coincides with the onset of 3D unidirectional CDW order.

The fact that we can clearly detect the onset of 3D unidirectional CDW order in the Seebeck coefficient allows us to examine whether it causes the FSR in YBCO. In Fig. 5(b), we plot S_a/T versus T at $p = 0.12$ for $H = 10$, 16, and 34 T. We see that S_a/T starts to deviate downward from its high-temperature behavior below $T \simeq 130$ K, it peaks at 105 K, and then it drops to become negative below $\sim$60 K. This is a gradual process, which starts in parallel with the gradual growth of short-range 2D CDW modulations seen in XRD below $\simeq$140 K [19]. (Down to T_c, both the Seebeck and the XRD intensity are independent of magnetic field.)

The decrease in S/T upon cooling is the signature of the FSR that leads to the formation of a small electron pocket in the Fermi surface at low temperature, detected via quantum oscillations, whose Fermi energy is consistent with the value of S/T at $T \to 0$ [Fig. 5(b)] [9]. In other words, the entire evolution of S_a/T versus T is quantitatively

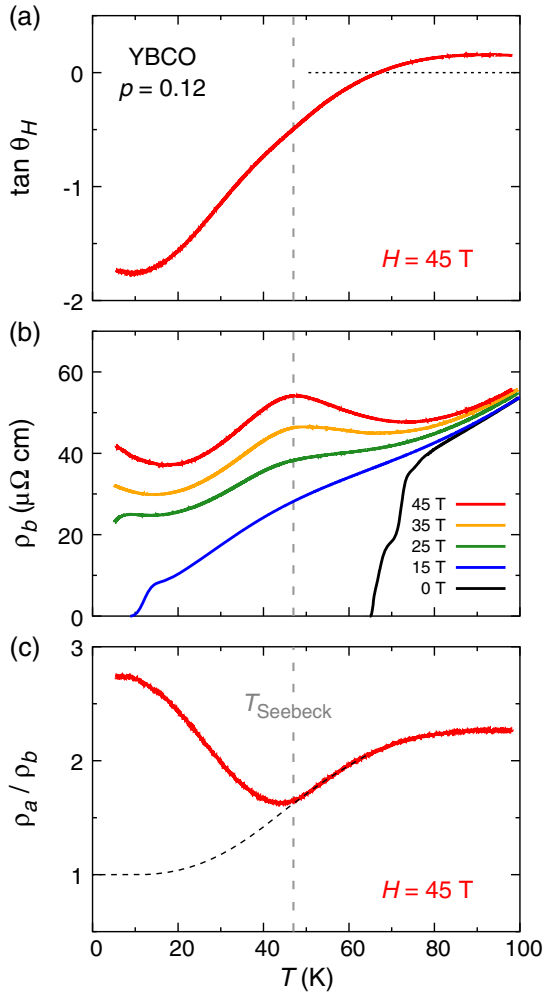

FIG. 6. (a) Tangent of the Hall angle, $\tan\theta_H \equiv \rho_{ab}/\rho_b$, in YBCO at $p = 0.12$, plotted versus temperature at $H = 45$ T, for a crystal with $J\|b$. The gray vertical dashed line in all three panels marks $T_{\text{Seebeck}} = 47$ K (Fig. 4). (b) Longitudinal resistivity ρ_b measured in the same sample (with $J\|b$), as a function of temperature for various magnetic fields as indicated. (c) In-plane anisotropy ratio, ρ_a/ρ_b, obtained from ρ_b in (b) and ρ_a measured with $J\|a$ in a separate, nominally identical detwinned single crystal of YBCO at $p = 0.12$. The dashed line in (c) is a guide to the eye showing the smooth decrease in ρ_a/ρ_b expected if the in-plane anisotropy would come from only the CuO chains, whose disorder level is much larger than that of the CuO_2 planes, giving $\rho_a/\rho_b \to 1.0$ as $T \to 0$.

consistent (in temperature and in amplitude) with a scenario whereby FSR is caused by the 2D CDW modulations (CDW-1). The fact that this evolution is completely unaffected by the sharp onset of the 3D unidirectional CDW order at 47 K, measured in YBCO at the same doping ($p = 0.12$) and the same field ($H = 16$ T) [27], indicates that it does not play a fundamental role in causing the FSR. It appears to only confer an extra anisotropy.

The picture obtained from thermoelectric measurements is quantitatively consistent with electric measurements of the longitudinal resistivity ρ_{xx} and Hall resistivity ρ_{xy}. In Fig. 6(a), we show the temperature dependence of the Hall angle ρ_{xy}/ρ_{xx} of YBCO at $p = 0.12$, measured at 45 T. We see that it decreases smoothly and monotonically below $T \simeq 100$ K, and becomes negative below $T \simeq 67$ K, in good agreement with the original study [6]. Note that ρ_{xy} becomes negative just above T_c, in a way that does not depend on field [6]. This is consistent with the fact that 2D CDW modulations are independent of field above T_c [19].

In Fig. 6(b), we show the temperature dependence of the b-axis resistivity at various fields. At 45 T, $\rho_b(T)$ exhibits a large peak, located precisely at T_{Seebeck}. In Fig. 6(c), the anisotropy ratio ρ_a/ρ_b is seen to undergo a substantial change below T_{Seebeck}, deviating upwards as $T \to 0$. This contrasts with the steady decline towards 1.0 one would expect if the anisotropy came only from the CuO chains, as these chains are much more disordered than the planes. We therefore infer that the reconstructed Fermi surface acquires in-plane anisotropy with the onset of unidirectional order below T_{Seebeck}, in its Fermi velocity and/or its scattering rate. Recent angle-dependent magnetoresistance measurements on YBCO at $p = 0.11$ have indeed revealed pronounced anisotropy of the electron pocket [39].

The fact that the 2D CDW modulations are bidirectional, i.e., that they run along both the a and b directions in the CuO_2 planes of YBCO, provides a natural mechanism for the formation of a small electron pocket in the reconstructed Fermi surface [24,25,40], located in nodal positions where the states are believed to be in underdoped cuprates with an antinodal pseudogap. An analysis of the anomalies in the sound velocities concluded that the order responsible for the observed transition must be bidirectional [29].

Note that the CDW modulations observed in Hg1201 [20] are very similar to the 2D CDW modulations in YBCO, and they cause a very similar FSR [41], with negative Hall and Seebeck coefficients at low temperature [10]. Therefore, attributing the cause of the FSR to these 2D CDW modulations is consistent with the fact that so far no field-induced 3D CDW order has been observed in Hg1201.

Given that 2D CDW modulations exist in the superconducting state at $H = 0$ [18,19], one might ask, Are there signatures of the FSR inside the superconducting phase, i.e., inside the green region of the H-T phase diagram (Fig. 4)? The answer is yes: in YBCO at $p = 0.11$, R_H at $T = 15$ K is negative for all fields down to $H = H_{\text{vs}} \simeq 10$ T, the field below which the vortex solid forms and $R_H = 0$ [36]. So a negative R_H is observed even when $H < H_{\text{Seebeck}}$. In the vortex-liquid state between H_{vs} and H_{c2}, the negative R_H could come from states inside the vortex core.

On the other hand, the thermal Hall conductivity κ_{xy} is dominated by d-wave quasiparticles outside the vortex cores. In YBCO at $p = 0.12$, κ_{xy} is negative in the normal state just above T_c [36], even in the limit $H = 0$, as is the electrical Hall conductivity [6]. Immediately below T_c, κ_{xy} becomes positive [36]. This sudden change of sign could be

due to a sudden increase in the quasiparticle mean-free path as the inelastic scattering is gapped out, as found in YBCO immediately below T_c [42]. Because the correlation length of the 2D CDW modulations is rather short in YBCO (and even shorter in Hg1201), the longer electronic mean-free path in the superconducting state may well average over the short-range CDW and wipe out the FSR. Increasing the field to suppress superconductivity makes κ_{xy} negative again [36]. The threshold field at which this change of sign happens coincides with H_{Seebeck} (Fig. 4), i.e., with the onset field for 3D CDW order. This can be understood as follows: 3D CDW order competes with superconductivity, its onset precipitates the demise of superconductivity, which causes a reduction in the mean-free path, making the FSR by short-range 2D CDW modulations possible again. In other words, 3D CDW order triggers the transition out of the superconducting phase and this is where κ_{xy} starts its transition from zero to its normal-state (negative) value [36].

V. SUMMARY

In summary, the Seebeck coefficient S of YBCO at $p = 0.11$ and 0.12 responds to two aspects of the complex CDW ordering in this material. First, as temperature is decreased from room temperature, S_a/T deviates gradually downward from its dependence at high temperature in parallel with the gradual growth in the 2D bidirectional CDW modulations detected by XRD well above T_c. S_a/T decreases below $T \simeq 100$ K to eventually become negative, extrapolating to a large negative value at $T \to 0$ that is quantitatively consistent with the small electron pocket in the normal-state Fermi surface detected by quantum oscillations at low temperature. The same monotonic decrease to negative values is observed in the Hall coefficient. We infer that the 2D bidirectional CDW modulations reconstruct the Fermi surface of YBCO, and produce the electron pocket. The same is true for Hg1201.

Second, a pronounced anomaly appears in S_b below a temperature and above a field that are both consistent with the onset temperature and field of the 3D unidirectional CDW order detected in YBCO by high-field XRD at $p = 0.11$ and 0.12. An additional in-plane anisotropy is also detected in the resistivity below the same onset temperature. We conclude that the extra anisotropy is due to that low-temperature order, which is not, however, the primary cause of the FSR. Nevertheless, given that the two types of CDW modulations (CDW-1 and CDW-2 in Fig. 4) have the same wavelength, they most likely have a common origin. It would be helpful to further elucidate the nature of their interplay.

ACKNOWLEDGMENTS

We would like to thank Johan Chang, Simon Gerber, Steve Kivelson, Wei-Sheng Lee, Cyril Proust and Marc-Henri Julien for stimulating and helpful discussions. A portion of this work was performed at the Laboratoire National des Champs Magnétiques Intenses of the CNRS, member of the European Magnetic Field Laboratory. Another portion of this work was performed at the National High Magnetic Field Laboratory, which is supported by the National Science Foundation Cooperative Agreement No. DMR-1157490, the State of Florida, and the U.S. Department of Energy. O. C.-C. was supported by a fellowship from the Natural Sciences and Engineering Research Council of Canada (NSERC). D. L. thanks Agence Nationale de Recherche (UNESCOS project ANR-14-CE05-0007), the Laboratoire d'Excellence LANEF (ANR-10-LABX-51-01), and the Université Grenoble-Alpes (SMIng-AGIR) for their support. L. T. thanks ESPCI-ParisTech, Université Paris-Sud, CEA-Saclay, and the Collège de France for their hospitality and support, and the European Research Council (Grant No. ERC-319286 QMAC) and LABEX PALM (ANR-10-LABX-0039-PALM) for their support, while this article was written. R. L., D. A. B., and W. N. H. acknowledge funding from the Natural Sciences and Engineering Research Council of Canada (NSERC). L. T. acknowledges support from the Canadian Institute for Advanced Research (CIFAR) and funding from the Natural Sciences and Engineering Research Council of Canada (NSERC; PIN:123817), the Fonds de recherche du Québec–Nature et Technologies (FRQNT), the Canada Foundation for Innovation (CFI), and a Canada Research Chair. Part of this work was funded by the Gordon and Betty Moore Foundation's EPiQS Initiative (Grant No. GBMF5306 to L. T.).

[1] L. Taillefer, *Fermi Surface Reconstruction in High-T_c Superconductors*, J. Phys. Condens. Matter **21**, 164212 (2009).

[2] N. Doiron-Leyraud, C. Proust, D. LeBoeuf, J. Levallois, J.-B. Bonnemaison, R. Liang, D. A. Bonn, W. N. Hardy, and L. Taillefer, *Quantum Oscillations and the Fermi Surface in an Underdoped High-T_c Superconductor*, Nature (London) **447**, 565 (2007).

[3] E. A. Yelland, J. Singleton, C. H. Mielke, N. Harrison, F. F. Balakirev, B. Dabrowski, and J. R. Cooper, *Quantum Oscillations in the Underdoped Cuprate* $YBa_2Cu_4O_8$, Phys. Rev. Lett. **100**, 047003 (2008).

[4] A. F. Bangura, J. D. Fletcher, A. Carrington, J. Levallois, M. Nardone, B. Vignolle, P. J. Heard, N. Doiron-Leyraud, D. LeBoeuf, L. Taillefer, S. Adachi, C. Proust, and N. E. Hussey, *Small Fermi Surface Pockets in Underdoped High Temperature Superconductors: Observation of Shubnikov–de Haas Oscillations in* $YBa_2Cu_4O_8$, Phys. Rev. Lett. **100**, 047004 (2008).

[5] N. Barišić, M. K. Chan, Y. Li, G. Yu, X. Zhao, M. Dressel, A. Smontara, and M. Greven, *Universal Sheet Resistance and Revised Phase Diagram of the Cuprate*

High-Temperature Superconductors, Proc. Natl. Acad. Sci. U.S.A. **110**, 12235 (2013).

[6] D. LeBoeuf, N. Doiron-Leyraud, J. Levallois, R. Daou, J.-B. Bonnemaison, N. E. Hussey, L. Balicas, B. J. Ramshaw, R. Liang, D. A. Bonn, W. N. Hardy, S. Adachi, C. Proust, and L. Taillefer, *Electron Pockets in the Fermi Surface of Hole-Doped High-T_c Superconductors*, Nature (London) **450**, 533 (2007).

[7] D. LeBoeuf, N. Doiron-Leyraud, B. Vignolle, M. Sutherland, B. J. Ramshaw, J. Levallois, R. Daou, F. Laliberté, O. Cyr-Choinière, J. Chang, Y. J. Jo, L. Balicas, R. Liang, D. A. Bonn, W. N. Hardy, C. Proust, and L. Taillefer, *Lifshitz Critical Point in the Cuprate Superconductor* $YBa_2Cu_3O_y$ *from High-Field Hall Effect Measurements*, Phys. Rev. B **83**, 054506 (2011).

[8] J. Chang, R. Daou, C. Proust, D. LeBoeuf, N. Doiron-Leyraud, F. Laliberté, B. Pingault, B. J. Ramshaw, R. Liang, D. A. Bonn, W. N. Hardy, H. Takagi, A. B. Antunes, I. Sheikin, K. Behnia, and L. Taillefer, *Nernst and Seebeck Coefficients of the Cuprate Superconductor* $YBa_2Cu_3O_{6.67}$*: A Study of Fermi Surface Reconstruction*, Phys. Rev. Lett. **104**, 057005 (2010).

[9] F. Laliberté, J. Chang, N. Doiron-Leyraud, E. Hassinger, R. Daou, M. Rondeau, B. J. Ramshaw, R. Liang, D. A. Bonn, W. N. Hardy, S. Pyon, T. Takayama, H. Takagi, I. Sheikin, L. Malone, C. Proust, K. Behnia, and L. Taillefer, *Fermi-Surface Reconstruction by Stripe Order in Cuprate Superconductors*, Nat. Commun. **2**, 432 (2011).

[10] N. Doiron-Leyraud, S. Lepault, O. Cyr-Choinière, B. Vignolle, G. Grissonnanche, F. Laliberté, J. Chang, N. Barišić, M. K. Chan, L. Ji, X. Zhao, Y. Li, M. Greven, C. Proust, and L. Taillefer, *Hall, Seebeck, and Nernst Coefficients of Underdoped* $HgBa_2CuO_{4+\delta}$*: Fermi-Surface Reconstruction in an Archetypal Cuprate Superconductor*, Phys. Rev. X **3**, 021019 (2013).

[11] T. Suzuki, T. Goto, K. Chiba, M. Minami, Y. Oshima, T. Fukase, M. Fujita, and K. Yamada, *Hall Coefficient of* $La_{1.88-y}Y_ySr_{0.12}CuO_4$ *($y = 0$, 0.04) at Low Temperatures under High Magnetic Fields*, Phys. Rev. B **66**, 104528 (2002).

[12] S. Badoux, S. A. A. Afshar, B. Michon, A. Ouellet, S. Fortier, D. LeBoeuf, T. P. Croft, C. Lester, S. M. Hayden, H. Takagi, K. Yamada, D. Graf, N. Doiron-Leyraud, and L. Taillefer, *Critical Doping for the Onset of Fermi-Surface Reconstruction by Charge-Density-Wave Order in the Cuprate Superconductor* $La_{2-x}Sr_xCuO_4$, Phys. Rev. X **6**, 021004 (2016).

[13] T. Noda, H. Eisaki, and S.-i. Uchida, *Evidence for One-Dimensional Charge Transport in* $La_{2-x-y}Nd_ySr_xCuO_4$, Science **286**, 265 (1999).

[14] M. Hücker, V. Kataev, J. Pommer, O. Baberski, W. Schlabitz, and B. Buchner, *Consequences of Stripe Order for the Transport Properties of Rare Earth Doped* $La_{2-x}Sr_xCuO_4$, J. Phys. Chem. Solids **59**, 1821 (1998).

[15] T. Adachi, T. Noji, and Y. Koike, *Crystal Growth, Transport Properties, and Crystal Structure of the Single-Crystal* $La_{2-x}Ba_xCuO_4$ *($x = 0.11$)*, Phys. Rev. B **64**, 144524 (2001).

[16] J. M. Tranquada, B. J. Sternlieb, J. D. Axe, Y. Nakamura, and S. Uchida, *Evidence for Stripe Correlations of Spins and Holes in Copper Oxide*, Nature (London) **375**, 561 (1995).

[17] J. Fink, V. Soltwisch, J. Geck, E. Schierle, E. Weschke, and B. Büchner, *Phase Diagram of Charge Order in* $La_{1.8-x}Eu_{0.2}Sr_xCuO_4$ *from Resonant Soft X-Ray Diffraction*, Phys. Rev. B **83**, 092503 (2011).

[18] G. Ghiringhelli, M. Le Tacon, M. Minola, S. Blanco-Canosa, C. Mazzoli, N. B. Brookes, G. M. De Luca, A. Frano, D. G. Hawthorn, F. He, T. Loew, M. Moretti Sala, D. C. Peets, M. Salluzzo, E. Schierle, R. Sutarto, G. A. Sawatzky, E. Weschke, B. Keimer, and L. Braicovich, *Long-Range Incommensurate Charge Fluctuations in* $(Y,Nd)Ba_2Cu_3O_{6+x}$, Science **337**, 821 (2012).

[19] J. Chang, E. Blackburn, A. T. Holmes, N. B. Christensen, J. Larsen, J. Mesot, Ruixing Liang, D. A. Bonn, W. N. Hardy, A. Watenphul, M. v. Zimmermann, E. M. Forgan, and S. M. Hayden, *Direct Observation of Competition between Superconductivity and Charge Density Wave Order in* $YBa_2Cu_3O_{6.67}$, Nat. Phys. **8**, 871 (2012).

[20] W. Tabis, Y. Li, M. Le Tacon, L. Braicovich, A. Kreyssig, M. Minola, G. Dellea, E. Weschke, M. J. Veit, M. Ramazanoglu, A. I. Goldman, T. Schmitt, G. Ghiringhelli, N. Barišić, M. K. Chan, C. J. Dorow, G. Yu, X. Zhao, B. Keimer, and M. Greven, *Charge Order and Its Connection with Fermi-Liquid Charge Transport in a Pristine High-*T_c *Cuprate*, Nat. Commun. **5**, 5875 (2014).

[21] T. P. Croft, C. Lester, M. S. Senn, A. Bombardi, and S. M. Hayden, *Charge Density Wave Fluctuations in* $La_{2-x}Sr_xCuO_4$ *and Their Competition with Superconductivity*, Phys. Rev. B **89**, 224513 (2014).

[22] A. J. Millis and M. R. Norman, *Antiphase Stripe Order as the Origin of Electron Pockets Observed in* 1/8*-Hole-Doped Cuprates*, Phys. Rev. B **76**, 220503 (2007).

[23] H. Yao, D.-H. Lee, and S. Kivelson, *Fermi-Surface Reconstruction in a Smectic Phase of a High-Temperature Superconductor*, Phys. Rev. B **84**, 012507 (2011).

[24] N. Harrison and S. E. Sebastian, *Fermi Surface Reconstruction from Bilayer Charge Ordering in the Underdoped High Temperature Superconductor* $YBa_2Cu_3O_{6+x}$, New J. Phys. **14**, 095023 (2012).

[25] A. Allais, D. Chowdhury, and S. Sachdev, *Connecting High-Field Quantum Oscillations to Zero-Field Electron Spectral Functions in the Underdoped Cuprates*, Nat. Commun. **5**, 5771 (2014).

[26] S. Gerber *et al.*, *Three-Dimensional Charge Density Wave Order in* $YBa_2Cu_3O_{6.67}$ *at High Magnetic Fields*, Science **350**, 949 (2015).

[27] J. Chang, E. Blackburn, O. Ivashko, A. T. Holmes, N. B. Christensen, M. Hucker, Ruixing Liang, D. A. Bonn, W. N. Hardy, U. Rutt, M. v. Zimmermann, E. M. Forgan, and S. M. Hayden, *Magnetic Field Controlled Charge Density Wave Coupling in Underdoped* $YBa_2Cu_3O_{6+x}$, Nat. Commun. **7**, 11494 (2016).

[28] H. Jang *et al.*, *Ideal Charge-Density-Wave Order in the High-Field State of Superconducting YBCO*, Proc. Natl. Acad. Sci. U.S.A. **113**, 14645 (2016).

[29] D. LeBoeuf, S. Kramer, W. N. Hardy, Ruixing Liang, D. A. Bonn, and C. Proust, *Thermodynamic Phase Diagram of Static Charge Order in Underdoped* $YBa_2Cu_3O_y$, Nat. Phys. **9**, 79 (2013).

[30] R. Liang, D. A. Bonn, and W. N. Hardy, *Growth of YBCO Single Crystals by the Self-Flux Technique*, Philos. Mag. **92**, 2563 (2012).

[31] R. Liang, D. A. Bonn, and W. N. Hardy, *Evaluation of* CuO_2 *Plane Hole Doping in* $YBa_2Cu_3O_{6+x}$ *Single Crystals*, Phys. Rev. B **73**, 180505 (2006).

[32] G. Grissonnanche *et al.*, *Direct Measurement of the Upper Critical Field in a Cuprate Superconductor*, Nat. Commun. **5**, 3280 (2014).

[33] Jing Fei Yu, B. J. Ramshaw, I. Kokanović, K. A. Modic, N. Harrison, James Day, Ruixing Liang, W. N. Hardy, D. A. Bonn, A. McCollam, S. R. Julian, and J. R. Cooper, *Magnetization of Underdoped* $YBa_2Cu_3O_y$ *Above the Irreversibility Field*, Phys. Rev. B **92**, 180509 (2015).

[34] K. Behnia, D. Jaccard, and J. Flouquet, *On the Thermoelectricity of Correlated Electrons in the Zero-Temperature Limit*, J. Phys. Condens. Matter **16**, 5187 (2004).

[35] C. Jaudet, D. Vignolles, A. Audouard, J. Levallois, D. LeBoeuf, N. Doiron-Leyraud, B. Vignolle, M. Nardone, A. Zitouni, R. Liang, D. A. Bonn, W. N. Hardy, L. Taillefer, and C. Proust, *de Haas–van Alphen Oscillations in the Underdoped High-Temperature Superconductor* $YBa_2Cu_3O_{6.5}$, Phys. Rev. Lett. **100**, 187005 (2008).

[36] G. Grissonnanche *et al.*, *Onset Field for Fermi-Surface Reconstruction in the Cuprate Superconductor YBCO*, arXiv:1508.05486.

[37] J. Chang, N. Doiron-Leyraud, O. Cyr-Choiniere, G. Grissonnanche, F. Laliberté, E. Hassinger, J-Ph. Reid, R. Daou, S. Pyon, T. Takayama, H. Takagi, and L. Taillefer, *Decrease of Upper Critical Field with Underdoping in Cuprate Superconductors*, Nat. Phys. **8**, 751 (2012).

[38] T. Wu, H. Mayaffre, S. Krämer, M. Horvatić, C. Berthier, P. L. Kuhns, A. P. Reyes, R Liang, W. N. Hardy, D. A. Bonn, and M.-H. Julien, *Emergence of Charge Order from the Vortex State of a High-Temperature Superconductor*, Nat. Commun. **4**, 2113 (2013).

[39] B. J. Ramshaw, N. Harrison, S. E. Sebastian, S. Ghannadzadeh, K. A. Modic, D. A. Bonn, W. N. Hardy, R. Liang, and P. A. Goddard, *Broken Rotational Symmetry on the Fermi Surface of a High-*T_c *Superconductor*, Quantum Mater. **2**, 8 (2017).

[40] S. E. Sebastian, N. Harrison, F. F. Balakirev, M. M. Altarawneh, P. A. Goddard, R. Liang, D. A. Bonn, W. N. Hardy, and G. G. Lonzarich, *Normal-State Nodal Electronic Structure in Underdoped High-*T_c *Copper Oxides*, Nature (London) **511**, 61 (2014).

[41] M. K. Chan, N. Harrison, R. D. McDonald, B. J. Ramshaw, K. A. Modic, N. Barišić, and M. Greven, *Single Reconstructed Fermi Surface Pocket in an Underdoped Single-Layer Cuprate Superconductor*, Nat. Commun. **7**, 12244 (2016).

[42] Y. Zhang, N. P. Ong, P. W. Anderson, D. A. Bonn, R. Liang, and W. N. Hardy, *Giant Enhancement of the Thermal Hall Conductivity* κ_{xy} *in the Superconductor* $YBa_2Cu_3O_7$, Phys. Rev. Lett. **86**, 890 (2001).